

Isolation Improvement with Electromagnetic Band Gap Surfaces

John Sandora

A new type of engineered surface called an electromagnetic band gap blocks current from flowing at microwave frequencies. One application of this metamaterial is to employ the surface amid electronic devices to improve the electromagnetic isolation between them. The different geometry features of the device's individual unit cells create extra inductances and capacitances for electromagnetic waves. When the unit cell is properly tuned, the aggregate surface will block incoming signals just as a band-stop filter will. This additional isolation allows radio-frequency receivers to operate in closer proximity to transmitters than a normal metal surface would permit.



An electromagnetic band gap (EBG) material is a periodic surface specifically designed to have certain electromagnetic properties at specific frequencies. The term “metamaterial” is sometimes used to describe such engineered surfaces. Metamaterials (“meta” means “beyond” in Greek) are man-made materials not found in nature and designed by placing tiny resonant structures at regularly spaced distances to create the appearance of a different bulk propagation medium [1]. As long as the inserted structures, called cells, are very small compared to the propagating wavelength, they can create a macroscopic effect on the electromagnetic wave as it passes through the new medium. Figure 1 depicts the engineered material's macro/micro “atomic” geometry approximation and the corresponding periodic unit cell. Desired electromagnetic properties can include specific values of permittivity, permeability, reflected phase, and index of refraction. If such media could be realized, then human beings could control the propagation of electromagnetic waves in previously unfeasible ways [1].*

EBGs are a class of metamaterials whose purpose is to highly impede electromagnetic propagation along the device's surface within the frequency band of operation known as a “band gap” (hence the name “electromagnetic band gap” material) [2]. In this sense, it is an artificially high-impedance surface and blocks current from flowing at microwave frequencies. In contrast, normal metals

* We are always bounded by the laws of physics—in this case Maxwell's equations. Metamaterials are merely different man-made materials for these same laws to act in.

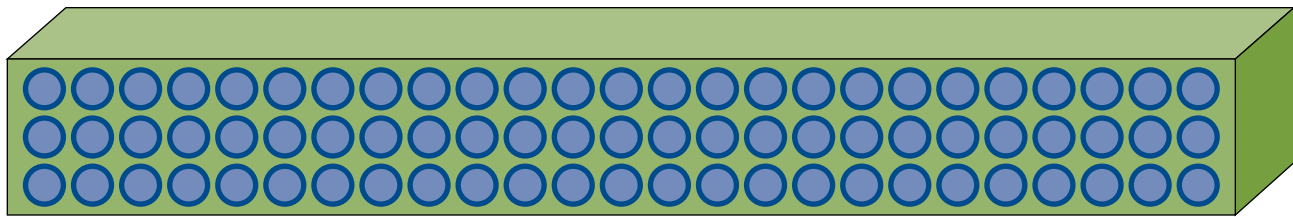


FIGURE 1. The bulk or macroscopic scale of the metamaterial is broken down into microcomponents in a repeated two-dimensional pattern. The physical properties of the microcomponents are the basis for the electromagnetic band gap (EBG) responses to radio-frequency propagation.

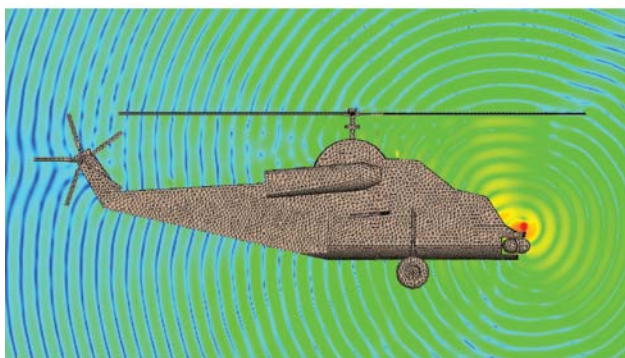
have very low impedance to current and allow it to flow over the entire metal surface. Impeding surface currents has immediate application to the field of antenna design, where metal ground planes have traditionally imposed constraints on both the minimum antenna size and corrupted the directivity pattern. The EBG was conceived as a potential solution by Daniel Sievenpiper and other researchers at the University of California at Los Angeles, who first constructed the unit cell geometry and investigated its properties [2].

This article describes another application of EBGs: employing the surface amid electronic devices to improve electromagnetic isolation between them. The small features of the periodic surface are easily manufactured by modern printed-circuit-board (PCB) companies. Computational analysis techniques such as the finite-element method (FEM) are shown to enable the design and optimization of the periodic unit cell geometry for particular frequency bands. Measured results show the comparison between bare metal, absorber materials, and EBG sur-

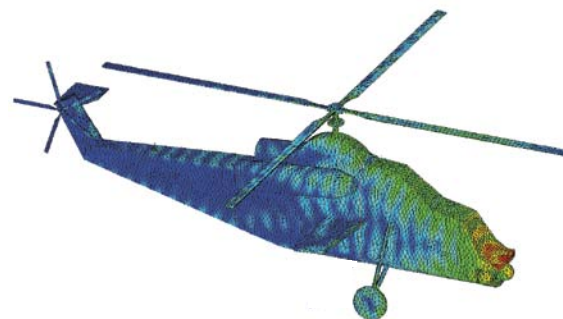
faces, and the EBG is shown to greatly improve isolation for realistic test cases.

Electromagnetic Interference

A common problem with electronic systems is a lack of electromagnetic isolation between closely spaced devices [3]. Modern military vehicles often contain several communication systems, early-warning receivers, radar, and radar jammers that are all in close proximity to each other. Metallic surfaces between transmitters and receivers allow current to propagate between systems with little impedance. Unfortunately, these systems can interfere with each other, causing major electromagnetic interference and electromagnetic compatibility issues that prevent the optimum operation of each individual system [3]. This problem is intensified by the vehicle body itself. Figure 2a shows a computer simulation of a snapshot in time of the electric-field intensity generated by a transmitting UHF antenna at the nose of a helicopter. Red indicates higher intensity; blue is



(a)



(b)

FIGURE 2. A numerical simulation for the electric-field intensity for a UHF transmitter on a helicopter nose (a) shows significant magnitudes throughout the air surrounding the entire helicopter. The electric-field intensity shown in (a) generates resulting currents in the helicopter itself (b). This current can cause interference with other onboard systems.

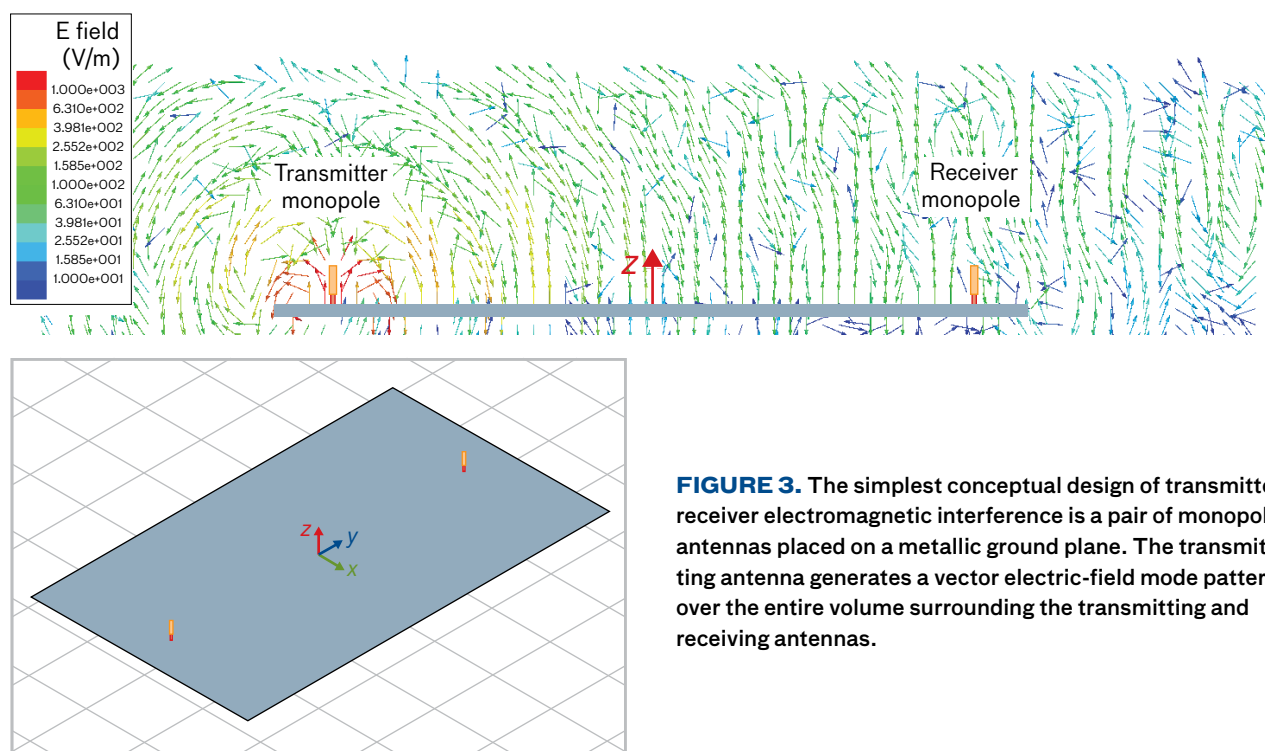


FIGURE 3. The simplest conceptual design of transmitter-receiver electromagnetic interference is a pair of monopole antennas placed on a metallic ground plane. The transmitting antenna generates a vector electric-field mode pattern over the entire volume surrounding the transmitting and receiving antennas.

the lowest intensity. These electromagnetic fields enable communication by radiating energy, but they also excite electric currents that run along the surface of the airframe. Figure 2b shows a similar snapshot in time of the electric-current intensity on the surface of the helicopter. It shows that these currents run along the entire airframe and will possibly interfere with other electromagnetic devices on board.

A simple abstraction of the interference problem is shown in Figure 3. A transmitter and a receiver are installed on a small rectangular metal conducting body. Suppose a high-power transmitter radiates energy out into the far field while a sensitive receiver nearby is listening for incoming signals. Energy will couple from one to the other as the electromagnetic fields assemble into specific patterns called “modes” and propagate along the surface. Maxwell’s equations dictate the specific mathematical relationships between the current, electric field, and magnetic field for all modes [4]. A full discussion is beyond the scope of this paper, but in general the modes are classified as

- **Transverse electric (TE)**—the electric field is completely perpendicular to the direction of propagation
- **Transverse magnetic (TM)**—the magnetic field is completely perpendicular to the direction of propagation

- **Transverse electromagnetic (TEM)**—both the electric and magnetic fields are completely perpendicular to the direction of propagation

Shown in Figure 3 is the simplest real-world case illustrating this problem. Two monopole antennas are installed onto the same metal ground plane and are separated by several wavelengths. The transmitter monopole on the left radiates the vector electric-field pattern shown in the upper figure. The metal body provides a coupling path from transmitter to receiver by allowing surface waves to propagate [5]. A conductor “shorts out” any electric fields parallel to its surface (TE mode) to zero, but the magnetic fields parallel to the surface (TM mode) are able to propagate just as easily with the conductor there as without. Interestingly, even somehow removing the metal ground plane would not fix the problem because electromagnetic waves are still able to propagate through thin air (TEM mode).

Traditionally, the solution to improving electromagnetic isolation has been to use electromagnetic absorbers to attenuate the waves as they travel. Electric fields are easily attenuated by low-conductivity materials such as carbon, but magnetic fields are a little more difficult to dissipate. The current state of the art is to use something called MAGRAM (magnetic radar-absorbing material),

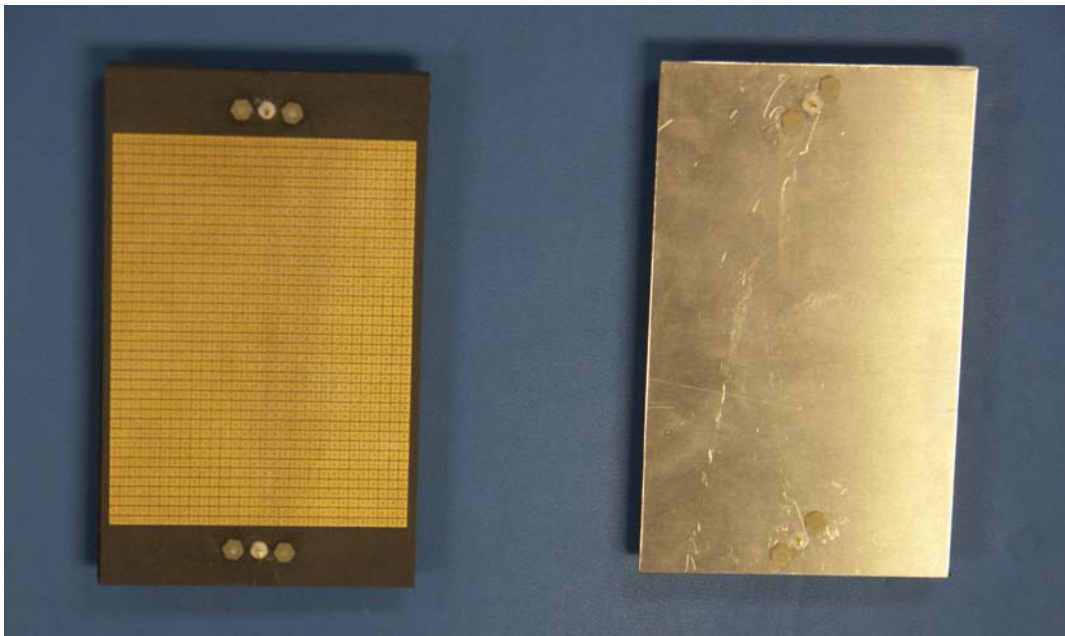


FIGURE 4. One example of an EBG textured-surface metamaterial is multiple cells with small gaps in two dimensions. On the right is shown a metal surface with the equivalent geometry to the EBG plate. In this configuration, the small dots centered at the top and bottom of the device are the transmitter/receiver pair. Each of these test boards is approximately 3 inches by 5 inches.

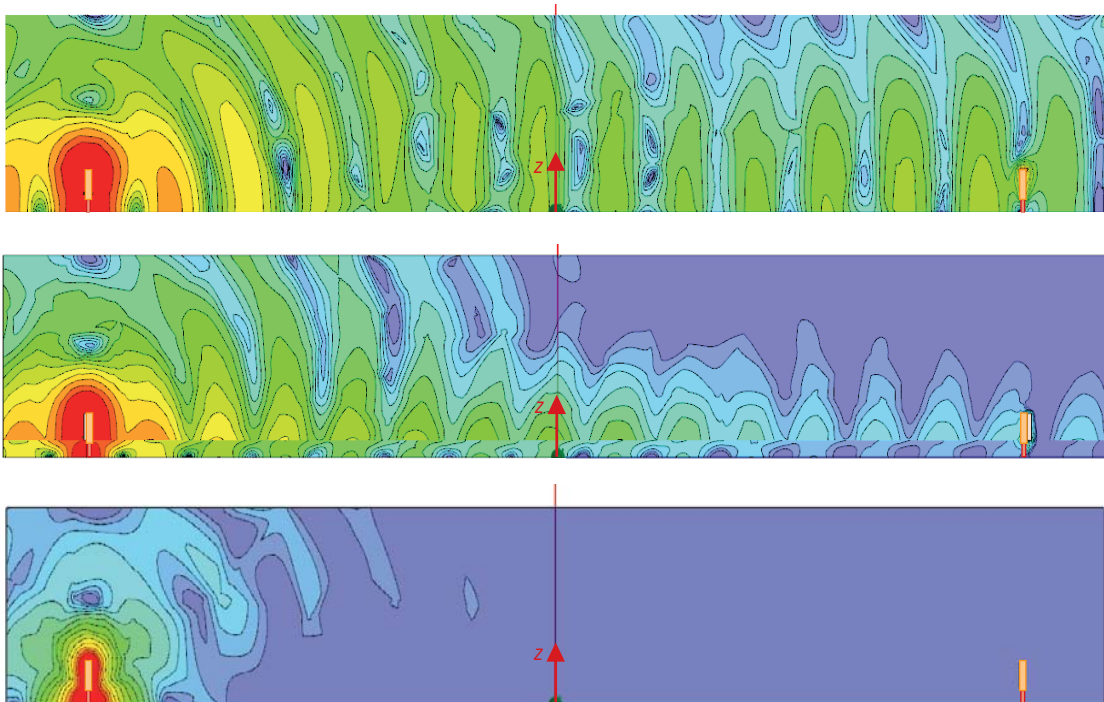


FIGURE 5. The electric-field intensity generated by the transmitting monopole (on the left) is shown for three cases: on a metal ground plane (top), with a MAGRAM absorber sheet (middle), and with an EBG surface (bottom). The improvements are clearly evident when MAGRAM is added to the ground plane and, more significantly, when EBG is present.

which consists of tiny iron beads encased in a thick rubber sheet [6]. The iron beads are densely packed throughout the sheet so that as the wave progresses, it excites eddy currents that run around the perimeter of each bead. Creating these extra currents takes additional energy so there is attenuation as the wave propagates through the material. MAGRAM's limitations are that it is heavy and not very effective over short distances. The solution presented next is an attempt to greatly improve isolation by blocking the waves from propagating at all.

Electromagnetic Band Gap Surfaces

An EBG structure is a new class of engineered surface. By carefully designing the texture of this surface, over the operating frequency range known as the band gap, we can do better than attenuating the waves—we can prevent them from propagating altogether [2]. Figure 4 shows an example EBG surface. Since we understand the modes that can transport energy, the concept of the surface development—adding specific textures onto the surface—can prevent these modes from being set up. If no modes are able to exist, electromagnetic energy cannot propagate. When faced with no other alternative, the electromagnetic waves lift up off the surface and radiate out into the surrounding space.

Figure 5 illustrates three relevant cases. First, the top image in Figure 5 shows a computer simulation of the electric-field intensity for the baseline case shown in Figure 3, two monopoles over a metal ground plane. The next image is of the electric-field intensity for the same geometry with a sheet of MAGRAM on top of the ground plane. The electric-field intensity decreases from left to right, indicating attenuation as the wave travels. The bottom image is for an EBG layer on top of the metal ground plane. In this case, the fields are shown to have extreme difficulty propagating along the surface, and instead radiate upwards away from the receiving monopole antenna. The color scale is the same for all three images.

Electromagnetic Analysis

The EBG structure, shown in Figure 4, is actually a simple unit cell repeated many times to form a surface. Each unit cell has three parts: the bottom metal ground plane layer, a square metal hat on top, and a conducting via between the two, as shown in Figure 6. The dimensions of the hat are carefully determined such that there is a specific gap

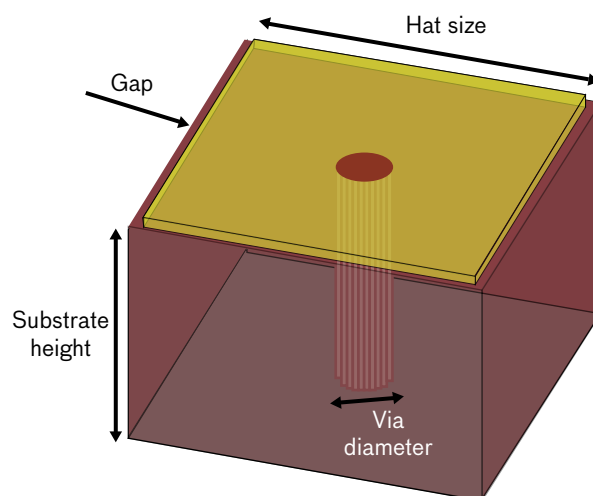


FIGURE 6. Individual EBG unit cell components are combined in two dimensions to create the surface. The hat size is slightly smaller than the substrate size. The gap dimensions versus hat size can be tuned to respond to appropriate frequency ranges.

in between neighbors in all directions. Although it is not required, a dielectric substrate usually exists between the two metal layers for both mechanical support and ease of fabrication with PCB techniques. Each unit cell's along-the-plane dimensions must be a small fraction of a wavelength in the operating range in order for the surface as a whole to appear electromagnetically homogeneous [7]. The unit cell dimensions are 2.25 mm for the hat length and width, along with a 0.38 mm diameter via. The gap between neighboring hats is 0.15 mm. The substrate used is a 4.1 mm thick version of a common radio-frequency (RF) PCB core called RO5880 (from the Rogers Corporation). It has a dielectric constant (ϵ_r) of 2.2 and a loss tangent ($\tan \delta$) of 0.002. This EBG was fabricated by etching away the gap regions of the copper on the top side of a RO5880 core. The conductive vias are “through holes” drilled and then plated through with nickel.

As stated previously, the EBG ability to block electromagnetic radiation transmission hinges upon having a unit cell such that it is impossible for any electromagnetic modes to exist on the surface. For certain geometry combinations of gap, height, and via diameter, radiation blockage is possible over a limited band gap frequency range. Interestingly, it is not necessary for the fields and current to be zero on every unit cell, nor is it required

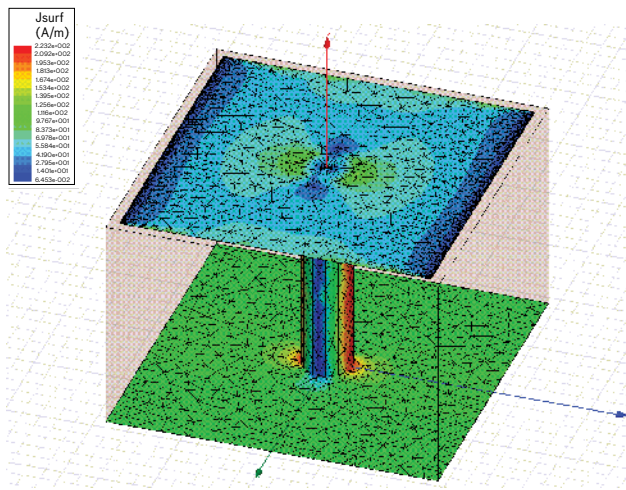


FIGURE 7. Finite-element analysis (FEM) of a single EBG unit cell is conducted over the top and bottom surfaces as well as the conducting via. Periodic boundary conditions set by the gaps between the cells speed up the process of full-surface analysis. FEM analysis is also performed in the vertical direction above each cell, as shown in Figure 8.

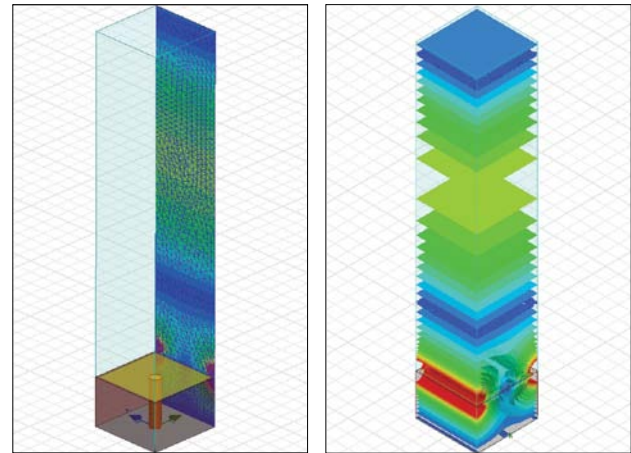


FIGURE 8. FEM analysis of the air above each unit cell shows the distribution of energy just above the surface. There is strong nearest-neighbor coupling on each side, but that energy will not propagate across the surface to the receiver antenna.

that there is no mutual coupling between cells. In fact, the gap between cells acts as a capacitance to the oncoming wave, and the via to ground provides an inductance. When the inductance and capacitance are properly tuned, the wave sees high-surface impedance similar to a band-stop-filter resonant circuit [7].

The EBG concept is proven by the use of computational electromagnetic techniques such as FEM. To analyze using the FEM, we need to discretize, or mesh, the geometry and solve for the current and fields by using a matrix solution of Maxwell's equations at every point on the mesh. Through the use of periodic boundary condi-

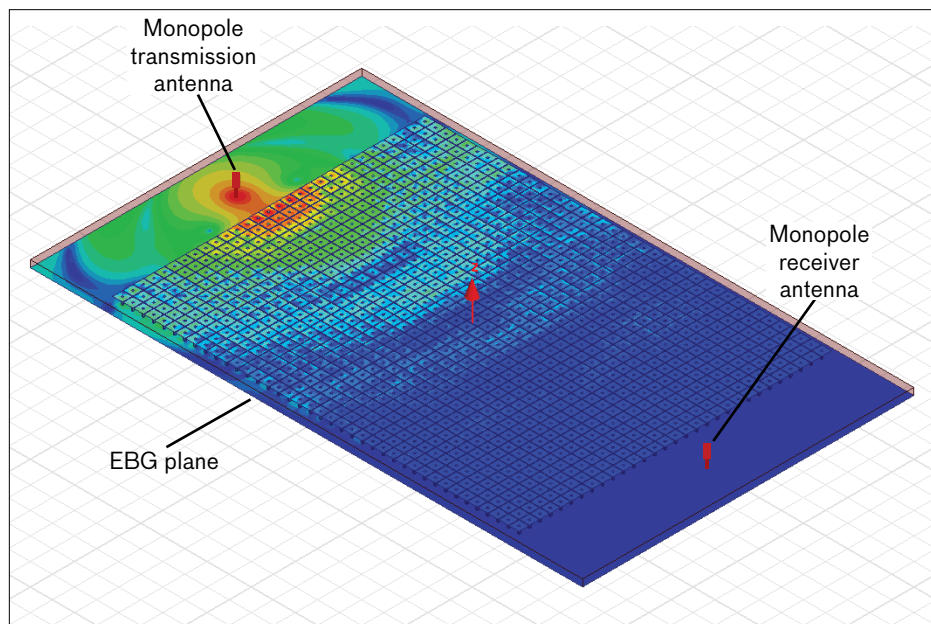


FIGURE 9. The results of FEM analysis are shown for a pair of monopoles (as in Figure 4), with an EBG surface separating the two. The significant decrease in propagation is evident.

tions on the unit cell walls, we can solve one unit cell virtually embedded in an infinitely large EBG surface [8]. Periodic boundary conditions allow for the solution of a single unit cell while still including mutual coupling effects from all neighboring cells [9]. Figure 7 shows an example mesh and current-intensity plot for the EBG unit cell for a single mode. Figures 8 and 9 illustrate the FEM analysis of the atmosphere above a unit cell and the resulting surface intensity, respectively. In order to improve the isolation for real-world systems and not merely illustrate an academic curiosity, we must ensure that all propagating modes are blocked. This requires solving for the currents and fields using the FEM to obtain a complete set of modes and determining which modes will propagate by using a dispersion diagram, such as the one shown in Figure 10.

A dispersion diagram is equivalent to the Bloch diagrams used to illustrate the energy-band structures in periodic crystalline media [10]. The two lowest-order modes shown in Figure 10 are plotted as curves of the frequency at which the mode occurs versus wave vector. The frequency band in between the two mode curves is where no modes can exist for a given wave vector; this is

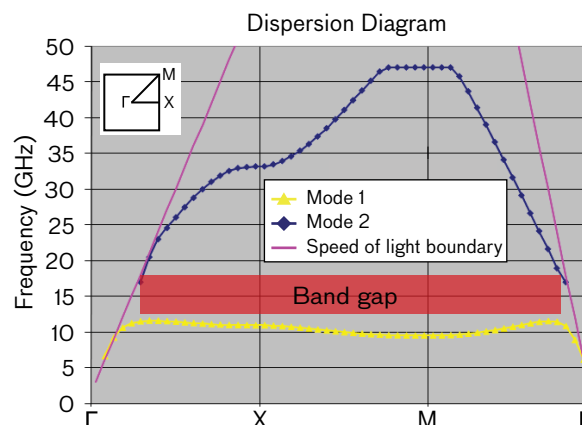


FIGURE 10. Conventional unit cell analysis produces a dispersion diagram showing the propagation modes and the associated band gap. Γ , X , and M are the wave vectors, and Mode 1 and Mode 2 are the transverse magnetic and transverse electric low-order eigenmodes.

the band gap. Although it is mathematically complete, one of the problems with the dispersion diagram is that it is computationally intensive. Because each point requires a full FEM solution, it therefore is not well suited for a practical design-flow procedure.

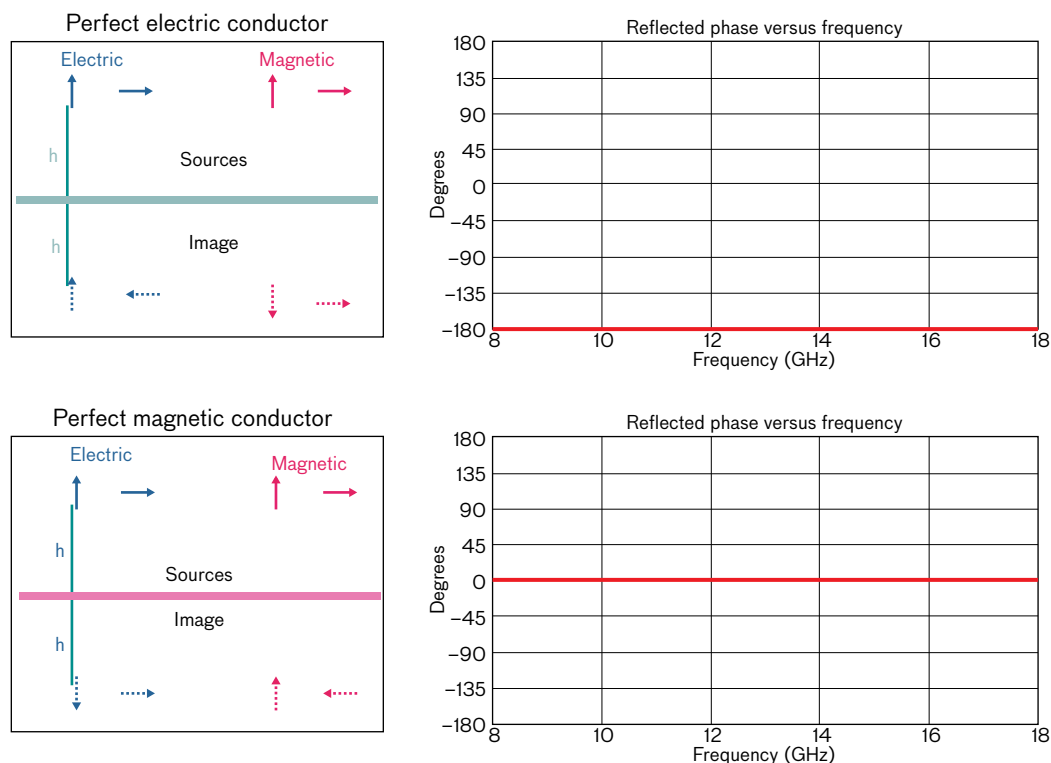


FIGURE 11. Electromagnetic image theory explains the in-phase and opposite-phase correlations between electric and magnetic fields at conducting surfaces [3].

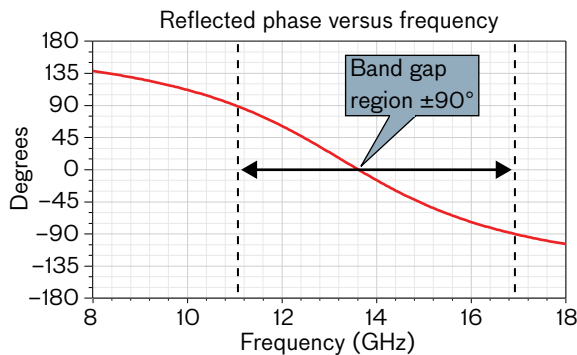


FIGURE 12. The reflected phase off an EBG surface crosses the 0° (perfectly in-phase) reflection point just as the theoretical magnetic conductor would.

An alternative process requires a single FEM solution of the unit cell and investigates the reflected phase. As electromagnetic waves bounce off a surface, they undergo a phase shift that depends on the electrical properties of the surface [11]. Figure 11 illustrates the image theory principle and reflection phase for perfect electric and magnetic conductors.

Basic electromagnetic boundary conditions determine that the reflection phase for a perfect electrical conductor (metal is a good approximation) is -180° for all frequencies [4]. In other words, the reflections off a metal surface are out of phase with the incident wave. Perfect

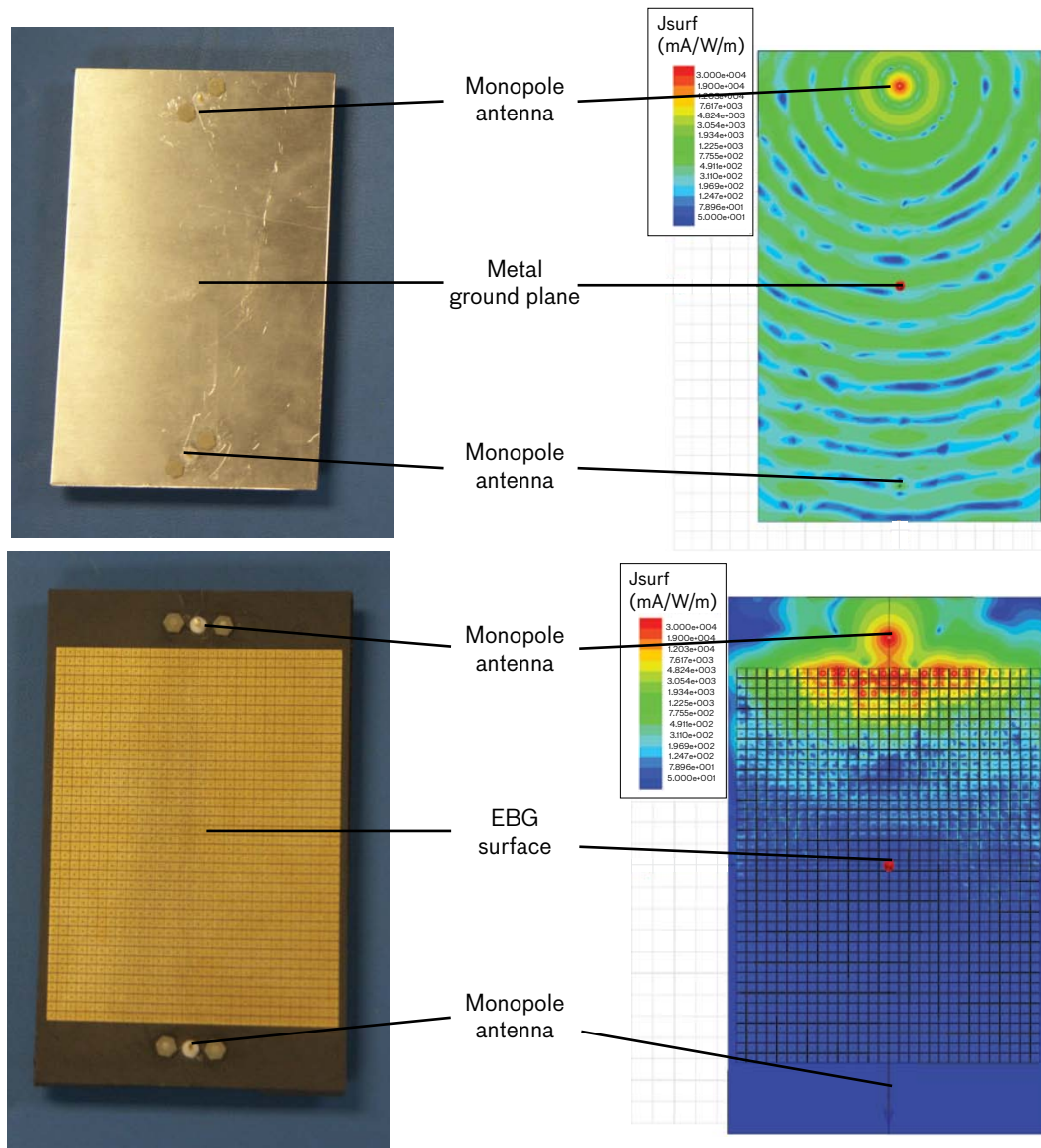


FIGURE 13. The analytical results on the EBG test board demonstrate the improvement over the metal ground plane. All experimental results in this research were closely matched to the FEM analysis calculations.

magnetic conductors do not exist in real life, but are only postulated in electromagnetic theory. If such a surface existed, it would have the property that reflected waves would have 0° phase shift and be perfectly in phase with the incident wave [4].

One of the reasons that EBGs have generated such excitement in the field of electromagnetics is because, within their band gap, they approximate certain characteristics of the purely theoretical magnetic conductor [2]. The theoretical becoming practical first becomes evident upon noting the reflected phase off an EBG surface as shown in Figure 12. The EBG appears to have reflected phase properties similar to the theoretical magnetic conductor. An alternative definition of the band gap could be the frequency range for which the reflected phase is within $\pm 90^\circ$, because within this frequency range the reflections off the EBG surface are at least partly in phase with the incident wave. As will be shown next, these $\pm 90^\circ$ frequency points map approximately onto the frequencies for which the EBG blocks surface waves. So although the reflection phase has interesting applications for low-profile antennas, which can be placed flat onto an EBG surface (and have their reflections still add up in phase), in this context it is an efficient design procedure for the isolation problem [12]. Now we have a simple way to determine the band gap frequencies accurately from a single unit cell simulation.

Isolation Improvement

The theoretical electromagnetic implications of textured surfaces discussed in the previous section have been an intense area of research in the academic community, but the practical benefits of having such a surface that can “block current” is very real-world. Through numerical simulations of the reflected phase, we have shown a simple way to determine the band gap range of frequencies from a single unit cell simulation. But simulating a realistic-sized EBG with thousands of unit cells is well beyond the capability of today’s computers. Therefore, accurately determining the isolation improvement that the EBG can provide must be determined experimentally.

Now that a straightforward design procedure has been found, the next step is to develop a test case to determine how well the EBG performs in the real world. Figure 13 shows the set of experimental conditions to measure the baseline isolation between two antennas. The top left image



FIGURE 14. Lincoln Laboratory’s millimeter-wave anechoic chamber is an ideal location to test the EBG’s capability of reducing or eliminating propagation between nearby monopole antennas. The electromagnetic shielding and interior wall configurations reduce the noise levels.

is a top-down view of the actual monopole antennas on a normal metal ground plane. The ground plane dimensions are 3 inches wide by 5 inches long, with a 4-inch spacing in between the two antennas. The right image is a current-intensity simulation for this baseline case.

The bottom left side of Figure 13 is the EBG test board. It has the same outer dimensions as the metal plate (3 × 5 inches) and has an identical metal ground plane, but the center 3.75 inches are now covered with EBG. The EBG test board’s current-intensity simulation is shown on the right. With the EBG surface present, the current now has extreme difficulty propagating across the board. With the current significantly decreased, the electromagnetic isolation between the two antennas is correspondingly increased, as proven in the following measurement.

Isolation measurements are performed inside an anechoic chamber to provide a controlled test environment. The chamber prevents outside signals from interfering with the measurement because the entire chamber is shielded. Pyramidal absorbers line the chamber walls to absorb reflections and bring the electromagnetic noise level down well below the signals of interest. These measurements were performed in the millimeter-wave anechoic chamber located at Lincoln Laboratory (Figure 14).

Isolation measurement results are shown in Figure 15. The figure shows the measured difference in decibel scale between the baseline and EBG test boards versus frequency. The red dotted line is at 0 dB, which is normalized to the baseline coupling level from the bare metal ground plane test case. The vertical orange dot-

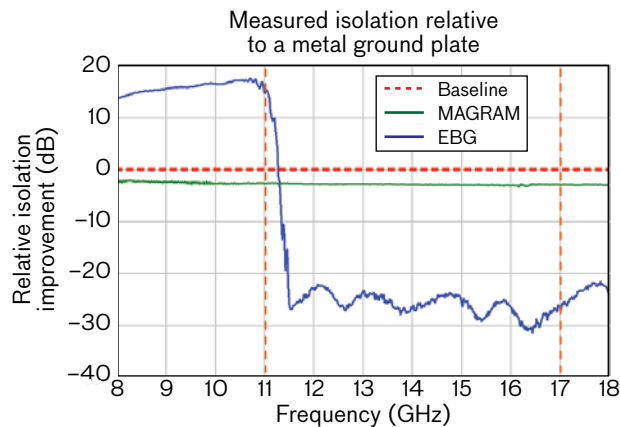


FIGURE 15. Isolation measurements of the planes shown in Figure 4 show the marked improvement of the EBG over both baseline metal and MAGRAM.

ted lines are at the $\pm 90^\circ$ phase frequencies found from the unit cell simulation. To the left of the first orange dotted line are the frequencies below the EBG region, and the positive values of the relative isolation indicate that there is stronger electromagnetic coupling in this region with the EBG than with the bare metal ground plane. Within the band gap region (between the two orange lines), the isolation has improved by more than 20 dB (a factor of 100 in linear scale). Negative numbers mean that less energy is coupled relative to the baseline case. Interestingly, past the right orange dotted line (the $+90^\circ$ degree reflection phase point), the isolation level is still improved. The band gap is the range over which

all modes are blocked, but some individual modes are rejected over a wider range. Over such a short distance (3.75 inches) a sheet of MAGRAM only improves isolation by approximately 3 dB (factor of 2).

Conclusion

The EBG has been shown to be remarkably effective at blocking surface waves from propagating over its band gap range of frequencies. The design presented here had a band gap from 11 to 17 GHz, approximately 43% of the center frequency. For other applications, the EBG unit cell may be scaled in size to operate at any frequency band: larger unit cells work for lower frequencies, and vice versa. EBG technology is presented here as an alternative to MAGRAM over limited frequency ranges. The EBG is still an active area of research in the field of electromagnetics. Extending its band gap range by using multilayer unit cell designs is the next step in EBG investigation. The PCB realization of these devices enables rapid verification of concepts, but eventually computational techniques will develop to where the entire EBG-coated body will be able to be analyzed. More practically, however, additional work must be done to improve the conformal coating process for real-world bodies. A conceptual example of a fully coated helicopter airframe is presented in Figure 16. Because the EBG is more effective than the current alternative, however, these obstacles will likely be overcome by many future electromagnetic systems looking to reduce their effect on, or the effects of, their neighboring systems.

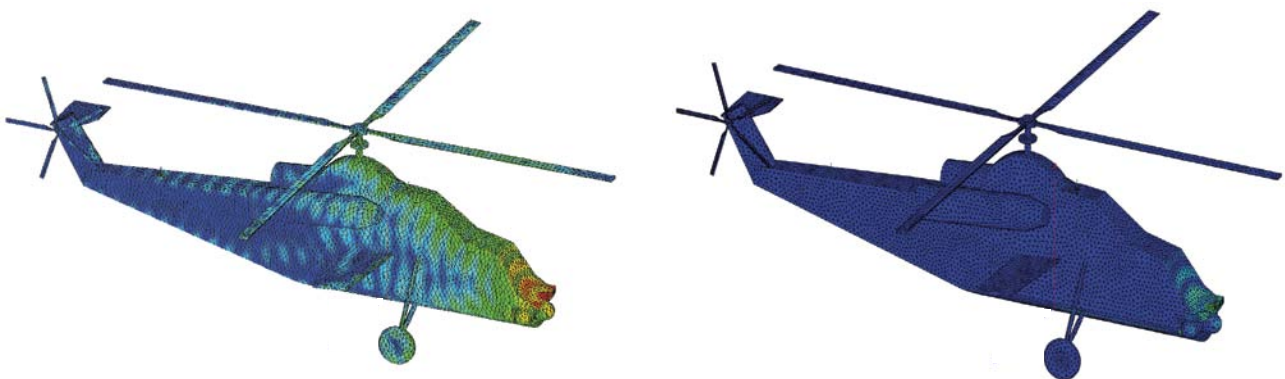


FIGURE 16. The larger test bodies show improvements in both MAGRAM (left) and EBG (right) surfaces, as expected, because of the longer separation between monopoles. Still, the EBG surface is clearly an improvement over MAGRAM and metal (baseline) surfaces.

Acknowledgments

The author would like to express his gratitude to David Mooradd for instructive technical discussions, practical advice, and measurements on the EBG test boards. He would also like to thank Sean Duffy, Jeffrey Herd, and Bradley Perry for advice on electromagnetic theory and simulation techniques. Matthew Cross provided PCB fabrication expertise for the test boards, and Dean Mailhot and Peter Priestner generously granted counsel on the measurement and practical application of the EBGs. ■

References

1. N. Engheta and R. Ziolkowski, eds., *Electromagnetic Metamaterials: Physics and Engineering Explorations*. New York: Wiley-IEEE Press, 2006.
2. D. Sievenpiper, L. Zhang, R.F.J. Broas, N.G. Alexopolous, and E. Yablonovitch, "High-Impedance Electromagnetic Surfaces with a Forbidden Frequency Band," *IEEE Transactions on Microwave Theory and Techniques*, vol. 47, no. 11, pp. 2059–2074, 1999.
3. "Electromagnetic Compatibility/Electromagnetic Interference." Clemson Vehicular Electronics Laboratory. <<http://www.cvel.clemson.edu/emc/>>, 31 March 2010.
4. C.A. Balanis, ed., *Advanced Engineering Electromagnetics*. International edition. New York: John Wiley and Sons, 1989.
5. R.F. Harrington, *Time-Harmonic Electromagnetic Fields* (IEEE Press Series on Electromagnetic Wave Theory). Revised edition. New York: Wiley-IEEE Press, 2001.
6. L.Z. Wu, J. Ding, H.B. Jiang, L.F. Chen, and C.K. Ong, "Particle Size Influence to the Microwave Properties of Iron Based Magnetic Particulate Composites," *Journal of Magnetism and Magnetic Materials*, vol. 285, no. 1–2, pp. 233–239, 2005.
7. S. Clavijo, R. E. Diaz, and W.E. McKinzie III, "Design Methodology for Sievenpiper High-Impedance Surfaces: An Artificial Magnetic Conductor for Positive Gain Electrically Small Antennas," *IEEE Transactions on Antennas and Propagation*, vol. 51, no. 10, pp. 2678–2690, 2003.
8. "Ansoft Electronic Design Products," Ansoft Ansys Product Suite, <<http://www.ansoft.com/>>, 31 March 2010.
9. D.S. Filipovic, J.L. Volakis, and L.S. Andersen, "Efficient Modeling and Analysis of Infinite Periodic Antenna Arrays by Tetrahedral Finite Elements," *Proceedings of the IEEE Antennas and Propagation Society International Symposium*, vol. 4, no. 8, pp. 2504–2507, 1999.
10. Y. Toyota, A.E. Engin, T.H. Kim, M. Swaminathan, and K. Uriu, "Stopband Prediction with Dispersion Diagram for Electromagnetic Bandgap Structures in Printed Circuit Boards," *Proceedings of the IEEE International Symposium on Electromagnetic Compatibility*, vol. 3, no. 8, pp. 807–811, 2006.
11. B.A. Munk, *Finite Antenna Arrays and FSS*. New York: Wiley-IEEE Press, 2003.
12. J.J. Lee, R.J. Broas, S. Livingston, and D. Sievenpiper, "Flush-Mounted Antennas on Hi-Z Ground Planes," *Proceedings of the IEEE Antennas and Propagation Society International Symposium*, vol. 3, pp. 764–767, 2002.



John Sandora is an associate technical staff member in the Air and Missile Defense Assessments Group. He earned bachelor's degrees in physics and electrical engineering in 2004 and a master's degree in electromagnetics in 2005 from the Ohio State University. After joining Lincoln Laboratory, he has continued working on radar, antenna design, and other projects involving advanced electromagnetics.